*MRS Communications (2018)*, *8*, 95–99
© Materials Research Society, 2018
doi:10.1557/mrc.2018.22

MRS Communications

Research Letter

# Silver nanostructures evolution in porous $SiO_2$/*p*-Si matrices for wide wavelength surface-enhanced Raman scattering applications

**Dmitry Yakimchuk, Egor Kaniukov** and **Victoria Bundyukova,** Division of Cryogenic Research, "Scientific-Practical Materials Research Center NAS of Belarus", Minsk 220072, Belarus
**Liubov Osminkina,** Department of Physics, Lomonosov Moscow State University, Leninskie Gory 1, Moscow 119991, Russian Federation
**Steffen Teichert,** Ernst Abbe University of Applied Science, Carl-Zeiss-Promenade 2, Jena 07745, Germany
**Sergey Demyanov,** Division of Cryogenic Research, "Scientific-Practical Materials Research Center NAS of Belarus", Minsk 220072, Belarus
**Vladimir Sivakov,** Functional Interfaces Department, Leibniz Institute of Photonic Technology, Albert Einstein St, 9, Jena 07745, Germany

Address all correspondence to Vladimir Sivakov at **vladimir.sivakov@leibniz-ipht.de**

(Received 22 January 2018; accepted 12 February 2018)

## Abstract

The formation of silver nanostructures (AgNSs) with different crystals morphology in porous $SiO_2$/*p*-Si templates by the electroless wet-chemical method at temperatures between 20 and 50 °C and surface-enhanced Raman scattering (SERS) was investigated. It was found that optimized dendritic silver architectures contain a significant number of localized "hot spots." We show that well-reproducible AgNSs provide a significantly enhanced Raman signal of Nile blue dye molecules up to $10^{-6}$ M by using different excitation wavelengths (473, 532, and 633 nm). Based on our observations, the well-organized AgNSs can act as efficient surfaces for SERS as well as (bio)-sensor applications.

## Introduction

Due to the fact that the shape of nanostructures (NSs) determines their physical properties, an active search for approaches, which provide possibility on controlling the NSs shape and dimension is nowadays being conducted.[1] One of the simplest approaches for controlling the NSs shape and localized growth is the using of porous matrices (templates) such as: $Al_2O_3$,[2,3] polymer films,[4–7] Si,[8] $SiO_2$,[9–11] $TiO_2$,[12,13] and other materials, in which the shape, dimensions, and position of the pores determine the geometry and localization on the surface of the produced NSs. Due to the highly developed silicon-based industry infrastructure, templates based on silicon and its derivatives have a great potential for practical usage. Silicon-based templates are important components in the creation of nano-, micro-, and magnetoelectronic devices.[14] The existing methods[15,16] for the synthesis of noble metal NSs using silicon-based templates make it possible to obtain sensor elements with an extremely high sensitivity to chemical and biologic media.[17,18] The nanosphere lithography and metal deposition methods based on colloidal crystal templating were suggested as alternative methods for the localized and selective noble metals formation.[19,20] In our previous work,[21] it was shown that using an external current source of a certain magnitude, the localized formation of copper dendrite-like NSs in the $SiO_2$/*n*-Si pores can be realized. The observed copper NSs found application as plasmon-active surfaces for amplification of the Raman scattering signal. However, the low local electric field enhancement factor of the copper NSs and surface degradation of such structures ("aging effect"—the rapid formation of oxides on the surface of structures) does not allow them to be seriously considered from the point-of-view of wide application in sensoric. For that reason, the application of gold or silver nanostructures (AgNSs) is more promising and favorable.[22]

Previously[23] we proposed a simple bottom-up method for localized AgNSs formation with precisely controlled AgNSs shape by varying the pore diameter by applying electroless wet-chemical deposition of metal into the $SiO_2$/*p*-Si pores template. At the same time, an important difference from other previously published works[2,24] is that the shape of the AgNSs does not reproduce the geometry of the pore, but can be varied widely: from faceted crystallites to dendritic-like structures. In particular, it was considered the formation of highly branched AgNSs, which can be an ideal surface for surface-enhanced Raman scattering (SERS). The advantage of such types of materials over colloidal nanoparticles, which are widespread today, is that the particles tend to form conglomerates, which makes the SERS signal unstable and poorly reproducible in a series of measurements.[25,26] Dendrites have a rigorous structure, which does not influence by adding the analyte solution. In addition, dendritic-like structures can provide a large number of "hot spots," which are the main cause of the high enhanced factor of the Raman scattering.[27] In the present paper, the dependence of the AgNSs shape on the deposition temperature of silver in the $SiO_2$/*p*-Si porous template is presented and discussed in details. The plasmonic activity of the silver



https://doi.org/10.1557/mrc.2018.22 Published online by Cambridge University Press

dendrites-like NSs was demonstrated experimentally in measurements of SERS activity of a highly dilute model dye molecule, i.e., Nile blue, deposited onto the silver dendrites in the $SiO_2$/*p*-Si porous templates.

## Methods

As templates for synthesis of AgNSs swift heavy ion-track[28] porous $SiO_2$ templates on *p*-type silicon substrate (12 Ωcm with (100) crystal orientation) were used with a silicon oxide layer thickness of 250 nm and pore sizes of 500 nm. The $SiO_2$/*p*-Si pore density over the surface was found to be $10^8$ $cm^{-2}$ according to the scanning electron microscopy (SEM) studies. The procedure of obtaining porous $SiO_2$/*p*-Si templates are described in our previous paper.[28] Silver deposition was carried out by electroless deposition from a solution of 0.02 M silver nitrate and 5 M hydrofluoric acid at ambient conditions. Before deposition, $4 \times 4$ $mm^2$ $SiO_2$/*p*-Si chips were treated with isopropyl alcohol and distilled water, and then dried in a stream of nitrogen to remove the adsorbed atmospheric residual from the surface. The growth of silver structures was carried out for 30 s at electrolyte temperature from 20 till 50 °C. At the end of the process, the samples were washed in distilled water and dried in air. The morphology of the $SiO_2$(Ag)/*p*-Si surface was studied using Carl Zeiss ULTRA 55, field emission scanning electron microscope.

The standard dye molecule—Nile blue was used to study the Raman signal enhancement induced by AgNSs in "dendrites-like" shape. To perform SERS measurements, 50 µl of an aqueous solution of Nile blue ($C_{20}H_{20}ClN_3O$) was dropped on the samples with "dendrites-like" NSs with an incubation time of 15 min, and subsequently rinsed in deionized water, and finally, dried in air. The Raman scattering measurements were performed at room temperature on a Nanofinder High End (Lotis TII, Belarus–Japan) confocal microscope-based setup. Lasers with wavelengths of 473, 532, and 633 nm were used as excitation source. The laser power at the samples' surface was kept at 50 µW and the typical single-spectrum acquisition time was 5 s. The backscattered light, not analyzed for its polarization, was dispersed using a spectrograph with 0.55 m focal lengths equipped with a 600 lines/mm single grating spectrometer with a spectral resolution around 3 $cm^{-1}$ and detected by a cooled CCD (charge-coupled device) camera. The laser beam was focused through a "50×" microscope objective lens. The resulting spot diameter was about 1 µm.

## Results and discussion

The self-organization of AgNSs in the porous $SiO_2$/*p*-Si templates occur with a high organization degree of pore filling at all process temperatures that were investigated by SEM as presented in Fig. 1. In addition, the silver deposit in the pores, independently of the process temperature, is characterized by the presence of clearly distinguished priority metal growth fronts along the pore walls. The predominant growth of silver along the edges of the pore is due to the presence of edge defects at the Si–$SiO_2$ boundary at the pore base, which are

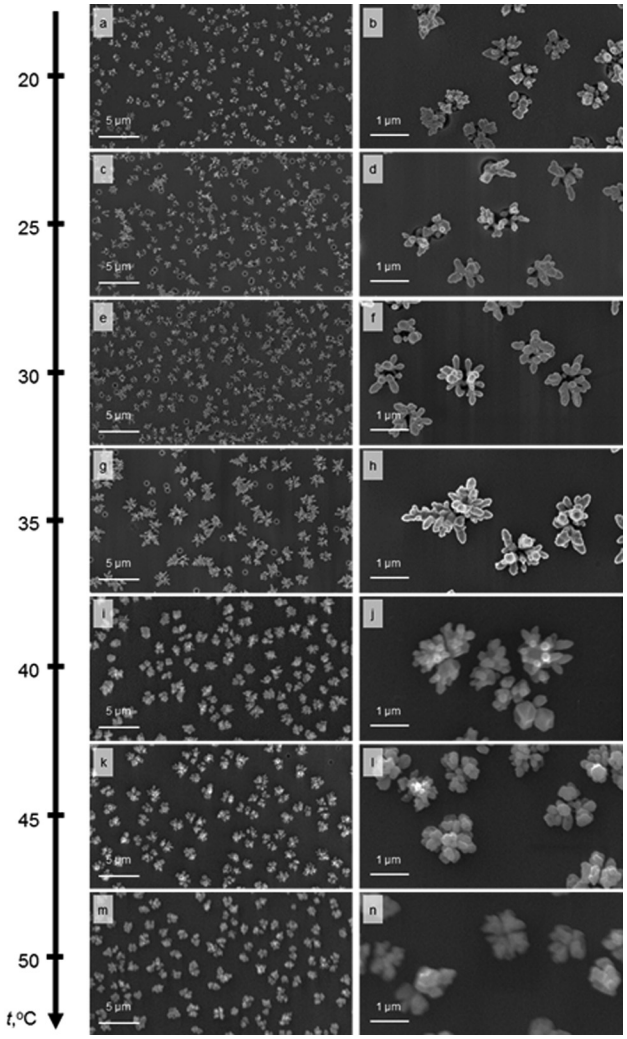



**Figure 1.** Scanning electron images of AgNSs morphology evolution in porous $SiO_2$/*p*-Si templates depending on the silver deposition temperature variation at: (a, b) 20 °C; (c, d) 25 °C; (e, f) 30 °C; (g, h) 35 °C; (i, j) 40 °C; (k, l) 45 °C; (m, n) 50 °C.

priority areas for nucleation of silver sediment at the initial stage of AgNSs formation. In this case, the middle of the pore in most cases remains partially unfilled that is clearly visible from SEM studies in Fig. 1.

The morphology of silver deposited at room temperature is characterized by some variation in the form of obtained AgNSs, which is manifested in the fact that part of the crystallites, which form part of the metallic sediment in the pores have faceted edges and another part have smoothed edges [Figs. 1(a) and 1(b)]. An increasing of silver deposition temperature to 25 °C leads to decreasing of the number of priority growth fronts with a simultaneous increasing of their lateral dimensions, while the structures are smoothed. Differences in the form of AgNSs over the surface are minimal as shown in Figs. 1(c) and 1(d). Further silver deposition temperature increasing to 30 °C does not lead any significant changes in


https://doi.org/10.1557/mrc.2018.22 Published online by Cambridge University Press

the morphology of the silver sediment in comparison to 25 °C, only insignificant increasing of its size was observed [Figs. 1(e) and 1(f)]. An increasing of the temperature of the solution to 35 °C leads to a radical change in the shape of the NSs: it occurs with an increase of dimensions with filling of the central part of the pore, while on the branches of the AgNSs appear branches of the second order and characteristic for "bud-like" facets of dendrites [Figs. 1(g) and 1(h)]. Further silver growth temperature increasing to 40 °C leads to the destruction of the dendritic structure and formation of AgNSs in different pores with different shapes: part of the metal deposit takes the form of faceted crystallites, and another part takes the form of the elongated smooth interconnected crystallites [Figs. 1(i) and 1(j)]. Further increasing of temperature leads to decreasing of the number of smooth elongated [Figs. 1(k) and 1(l)] crystallites at 45 °C with their complete degeneracy at 50 °C [Figs. 1(m) and 1(n)].

The SERS capabilities of the AgNSs in porous $SiO_2$/*p*-Si templates can easily be performed by a simple model SERS experiments using the dye molecule (Nile blue) as an agent of interest (analyte). The gaps between the dendrite branches [Fig. 2(a)] and the "bud-like" facets [Fig. 2(b)] are those nanoscale regions for which "hot spot" formation is characteristic.[27,29–31] Such structures are highly interesting for SERS applications. As it is known, the position of maximums of plasmonic structures extinction depends not only on their shape and size, but also on the polarization of the radiation, which induces plasmon oscillations.[1,29] Accordingly, the same effects will be achieved, when the spatial orientation of the plasmonic structure changes: inclination, turning, etc. SEM images in Fig. 2 show that the resulting structures and their components (individual trunks and branches) are not characterized by strict spatial orientation relative to the template, but have a chaotic inclination and are not identical copies of each other. It is known that dendrites have a large set of "hot spots".[27,30] Thus, taking into account the influence of the polarization of the exciting radiation on the distribution of plasmons along the dendrite,[29] it can be assumed that even a single silver structure has not one

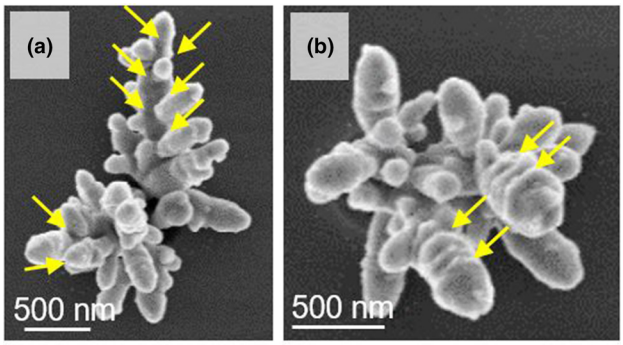



**Figure 2.** SEM images of localized regions with "hot spots" on the surface of AgNSs grown at 35 °C in the pores of the $SiO_2$/*p*-Si template: connecting parts of the branches (a) and the "bud-like" facets (b) of the dendrite.

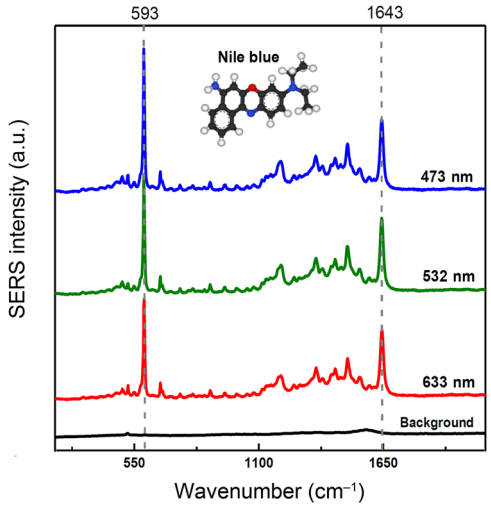



**Figure 3.** Normalized SERS spectra of the Nile blue molecule with a concentration of $10^{-6}$ M, obtained on the surface of AgNSs grown at 35 °C in the pores of the $SiO_2$/*p*-Si template, excited by using different excitation wavelengths (473, 532, and 633 nm), and the Raman spectrum of the substrate's background.

or several distinct bands of plasmon resonance. They are present in large numbers and are distributed throughout the long-wave interval corresponding to plasmon resonance bands of all possible AgNSs.[32]

Based on the obtained results, it can be proposed that such structures under consideration are suitable for using in SERS applications. This assumption was verified on $SiO_2$(Ag)/*p*-Si structures with dendrites in a series of SERS measurements using lasers with different wavelengths: blue (473 nm), green (532 nm), and red (633 nm), as shown in Fig. 3.

The SERS spectra of Nile blue with a concentration of $10^{-6}$ M have brightly expressed characteristic peaks at 592 and 1643 $cm^{-1}$ (Fig. 3), which correspond to the characteristic lines of Nile blue.[33,34] The intensity of the signal, when lasers with different wavelengths were used, indicates that the "hot spots" in the spectral region of 473–633 nm are uniformly distributed over the position and intensity of the plasmon resonance. A detailed study of this phenomenon with using of mathematical modeling with the interaction of an external electromagnetic wave with dendrites of different spatial orientations is planned to be carried out in the future work.

## Conclusions

AgNSs are formed in the porous $SiO_2$/*p*-Si template and the interrelation of their morphology with the deposition temperature was determined. It was found that at the temperature of 35 °C the most preferable AgNSs for SERS structures (highly branched dendrites) can be realized. The presence of gaps between the dendrite branches and the "bud-like" facets indicates the presence of "hot spots" in dendritic NSs. Highly reproducible morphology and pore localized synthesis of the



https://doi.org/10.1557/mrc.2018.22 Published online by Cambridge University Press

silver dendritic NSs in the $SiO_2$/*p*-Si templates allows one to obtain the SERS-active substrates working in a broad spectral range (473–633 nm). These surfaces are expected to appeal to a wide audience in the nanotechnology related fields, like environmental science, food science, and nanotoxicology, etc., due to the high potential for in-depth studies of substances and track it behavior. From the practical point of view, such silver dendrite NSs in porous $SiO_2$/*p*-Si matrices are highly perspective for cancer theranostics, food and environment monitoring, e.g., determination of pesticides or harmful additives, water pollution control, and other fields where precise analysis of components in the substances is required.

## Acknowledgments

This work was supported by the Scientific-technical 'program Technology-SG' (project number 3.1.5.1). VS gratefully acknowledged the German Federal Ministry of Education and Research (BMBF) in the frame of Baltic Sea Network "NanoPhoto" under Grant No. 01DS14017 and National Science Foundation of Germany (DFG) under Grant No. SI-1893/2-1 for the financial support. LAO gratefully acknowledged the Russian Science Foundation (Grant no. 17-12-01386) for the financial support.

## References

1. Z.L. Yang, Q.H. Li, F.X. Ruan, Z.P. Li, B. Ren, H.X. Xu, and Z.Q. Tian: FDTD for plasmonics: Applications in enhanced Raman spectroscopy. *Chin. Sci. Bull.* **55**, 2635–2642 (2010).
2. A. Spende, N. Sobel, M. Lukas, R. Zierold, J.C. Riedl, L. Gura, I. Schubert, J.M.M. Moreno, K. Nielsch, B. Stühn, C. Hess, C. Trautmann, and M.E. Toimil-Molares: $TiO_2$, $SiO_2$, and $Al_2O_3$ coated nanopores and nanotubes produced by ALD in etched ion-track membranes for transport measurements. *Nanotechnology* **26**, 335301 (2015).
3. N.A. Kalanda, G.G. Gorokh, M.V. Yarmolich, A.A. Lozovenko, and E.Y. Kanyukov: Magnetic and magnetoresistive properties of $Al_2O_3$–$Sr_2FeMoO_6$–δ–$Al_2O_3$ nanoheterostructures. *Phys. Solid State* **58**, 351–359 (2016).
4. P. Guo, C.R. Martin, Y. Zhao, J. Ge, and R.N. Zare: General method for producing organic nanoparticles using nanoporous membranes. *Nano Lett.* **10**, 2202–2206 (2010).
5. C. Shen, X. Wang, W. Zhang, and F. Kang: Direct prototyping of patterned nanoporous carbon: a route from materials to on-chip devices. *Sci. Rep.* **3**, 2294 (2013).
6. E.Y. Kaniukov, E.E. Shumskaya, D.V. Yakimchuk, A.L. Kozlovskiy, M.A. Ibragimova, and M.V. Zdorovets: Evolution of the polyethylene terephthalate track membranes parameters at the etching process. *J. Contemp. Phys.* (*Armenian Acad. Sci.*) **52**, 155–160 (2017).
7. A.L. Kozlovskiy, I.V. Korolkov, G. Kalkabay, M.A. Ibragimova, A.D. Ibrayeva, M.V. Zdorovets, V.S. Mikulich, D.V. Yakimchuk, A.E. Shumskaya, and E.Y. Kaniukov: Comprehensive study of Ni nanotubes for bioapplications: from synthesis to payloads attaching. *J. Nanomater.* **2017**, 1–9 (2017).
8. L. Boarino, S. Borini, and G. Amato: Electrical properties of mesoporous silicon: from a surface effect to coulomb blockade and more. *J. Electrochem. Soc.* **156**, K223–K226 (2009).
9. A. Dallanora, T.L. Marcondes, G.G. Bermudez, P.F.P. Fichtner, C. Trautmann, M. Toulemonde, and R.M. Papaléo: Nanoporous $SiO_2$/Si thin layers produced by ion track etching: dependence on the ion energy and criterion for etchability. *J. Appl. Phys.* **104**, 24307–1–24307-8 (2008).
10. H. Nishiyama, M. Mizoshiri, Y. Hirata, and J. Nishii: Hybrid microlens structures using femtosecond laser nonlinear lithography. *IOP Conf. Ser. Mater. Sci. Eng.* **18**, 1–4 (2011).
11. D. Fink, A.V. Petrov, K. Hoppe, W.R. Fahrner, R.M. Papaleo, A. S. Berdinsky, A. Chandra, A. Chemseddine, A. Zrineh, A. Biswas, F. Faupel, and L.T. Chadderton: Etched ion tracks in silicon oxide and silicon oxynitride as charge injection or extraction channels for novel electronic structures. *Nucl. Instrum. Methods Phys. Res. B* **218**, 355–361 (2004).
12. A. Cultrera, L. Boarino, G. Amato, and C. Lamberti: Band-gap states in unfilled mesoporous nc-$TiO_2$: measurement protocol for electrical characterization. *J. Phys. D Appl. Phys.* **47**, 015102 (1–8) (2014).
13. C.M. Han, T.S. Jang, H.E. Kim, and Y.H. Koh: Creation of nanoporous $TiO_2$ surface onto polyether ether ketone for effective immobilization and delivery of bone morphogenetic protein. *J. Biomed. Mater. Res. A* **102**, 1–39 (2014).
14. S. Demyanov, E. Kaniukov, A. Petrov, and V. Sivakov: Positive magnetoresistive effect in Si/$SiO_2$(Cu/Ni) nanostructures. *Sens. Actuators A, Phys.* **216**, 64–68 (2014).
15. A.Y. Panarin, S.N. Terekhov, K.I. Kholostov, and V.P. Bondarenko: SERS-active substrates based on n-type porous silicon. *Appl. Surf. Sci.* **256**, 6969–6976 (2010).
16. H. Bandarenka, K. Artsemyeva, S. Redko, A. Panarin, S. Terekhov, and V. Bondarenko: Effect of swirl-like resistivity striations in n+-type Sb doped Si wafers on the properties of Ag/porous silicon SERS substrates. *Phys. Status Solidi* **10**, 624–627 (2013).
17. K. Girel, E. Yantcevich, G. Arzumanyan, N. Doroshkevich, and H. Bandarenka: Detection of DNA molecules by SERS spectroscopy with silvered porous silicon as an active substrate. *Phys. Status Solidi* **213**, 2911–2915 (2016).
18. G. Arzumanyan, N. Doroshkevich, K. Mamatkulov, S. Shashkov, K. Girel, H. Bandarenka, and V. Borisenko: Phospholipid detection by surface-enhanced Raman scattering using silvered porous silicon substrates. *Phys. Status Solidi* **214**, 1600915 (2017).
19. M. Bechelany, P. Brodard, L. Philippe, and J. Michler: Extended domains of organized nanorings of silver grains as surface-enhanced Raman scattering sensors for molecular detection. *Nanotechnology* **20**, 455302 (2009).
20. S. Sakamoto, L. Philippe, M. Bechelany, J. Michler, H. Asoh, and S. Ono: Ordered hexagonal array of Au nanodots on Si substrate based on colloidal crystal templating. *Nanotechnology* **19**, 405304 (2008).
21. E. Kaniukov, D. Yakimchuk, G. Arzumanyan, H. Terryn, K. Baert, A. Kozlovskiy, M. Zdorovets, E. Belonogov, and S. Demyanov: Growth mechanisms of spatially separated copper dendrites in pores of a $SiO_2$ template. *Philos. Mag.* **97**, 2268–2283 (2017).
22. J. Baniukevic, I. Hakki Boyaci, A. Goktug Bozkurt, U. Tamer, A. Ramanavicius, and A. Ramanaviciene: Magnetic gold nanoparticles in SERS-based sandwich immunoassay for antigen detection by well oriented antibodies. *Biosens. Bioelectron.* **43**, 281–288 (2013).
23. V. Sivakov, E.Y. Kaniukov, A.V. Petrov, O.V. Korolik, A.V. Mazanik, A. Bochmann, S. Teichert, I.J. Hidi, A. Schleusener, D. Cialla, M. Eugenia Toimil-Molares, C. Trautmann, J. Popp, and S.E. Demyanov: Silver nanostructures formation in porous Si/$SiO_2$ matrix. *J. Cryst. Growth* **400**, 21–26 (2014).
24. A.E. Shumskaya, E.Y. Kaniukov, A.L. Kozlovskiy, D.I. Shlimas, M.V. Zdorovets, M.A. Ibragimova, V.S. Rusakov, and K.K. Kadyrzhanov: Template synthesis and magnetic characterization of FeNi nanotubes. *Prog. Electromagn. Res. C* **75**, 23–30 (2017).
25. X. Dou, Y.M. Jung, Z.Q. Cao, and Y. Ozaki: Surface-enhanced Raman scattering of biological molecules on metal colloid II: effects of aggregation of gold colloid and comparison of effects of pH of glycine solutions between gold and silver colloids. *Appl. Spectrosc.* **53**, 1440–1447 (1999).
26. O. Siiman, and H. Feilchenfeld: Internal fractal structure of aggregates of silver particles and its consequences on surface-enhanced Raman scattering intensities. *J. Phys. Chem.* **92**, 453–464 (1988).
27. H.J. Yin, Z.Y. Chen, Y.M. Zhao, M.Y. Lv, C.A. Shi, Z.L. Wu, X. Zhang, L. Liu, M.L. Wang, and H.J. Xu: Ag@Au core-shell dendrites: a stable, reusable and sensitive surface enhanced Raman scattering substrate. *Sci. Rep.* **5**, 1–9 (2015).


https://doi.org/10.1557/mrc.2018.22 Published online by Cambridge University Press

28. E.Y. Kaniukov, J. Ustarroz, D.V. Yakimchuk, M. Petrova, H. Terryn, V. Sivakov, and A.V. Petrov: Tunable nanoporous silicon oxide templates by swift heavy ion tracks technology. *Nanotechnology* **27**, 115305 (2016).
29. C. Feng, Y. Zhao, and Y. Jiang: Silver nano-dendritic crystal film: a rapid dehydration SERS substrate of totally new concept. *RSC Adv.* **5**, 4578–4585 (2015).
30. B. Zhao, Y. Lu, C. Zhang, Y. Fu, S. Moeendarbari, S.R. Shelke, Y. Liu, and Y. Hao: Silver dendrites decorated filter membrane as highly sensitive and reproducible three dimensional surface enhanced Raman scattering substrates. *Appl. Surf. Sci.* **387**, 431–436 (2016).
31. T. Qiu, Y. Zhou, J. Li, W. Zhang, X. Lang, T. Cui, and P.K. Chu: Hot spots in highly Raman-enhancing silver nano-dendrites. *J. Phys. D, Appl. Phys.* **42**, 175403 (2009).
32. B. Sharma, R.R. Frontiera, A.-I. Henry, E. Ringe, and R.P. Van Duyne: SERS: materials, applications, and the future. *Mater. Today* **15**, 16–25 (2012).
33. W.H. Li, R. Zamani, P. Rivera Gil, B. Pelaz, M. Ibanez, D. Cadavid, A. Shavel, R.A. Alvarez-Puebla, W.J. Parak, J. Arbiol, and A. Cabot: CuTe nanocrystals: shape and size control, plasmonic properties, and use as SERS probes and photothermal agents. *J. Am. Chem. Soc.* **135**, 7098 (2013).
34. P.G. Etchegoin and E.C. Le Ru: Resolving single molecules in surface-enhanced Raman scattering within the inhomogeneous broadening of Raman peaks. *Anal. Chem.* **82**, 2888–2892 (2010).



https://doi.org/10.1557/mrc.2018.22 Published online by Cambridge University Press